

05

## Control of spin wave characteristics in the system of YIG microwaveguides with various dipole coupling parameters

© A.B. Khutieva, V.R. Akimova, A.V. Sadovnikov

Chernyshevsky Saratov National Research State University,  
Saratov, Russia

E-mail: abkhutieva@gmail.com

Received July 19, 2023

Revised September 6, 2023

Accepted September 7, 2023

The propagation of spin waves (SW) in a bilayer array of laterally and vertically coupled microwaveguides is investigated. Using micromagnetic modeling, the spatial intensity distribution and dynamic magnetization distribution of SWs in an array of microwaveguides formed by iron-yttrium garnet (YIG) strips. Methods of control of the spatial structure of the spin-wave beam and its division between the channels of the array of the YIG microwaveguides. It is shown that it is possible to control the direction of propagation of the SW in an array of laterally and vertically coupled microwaveguides laterally and vertically coupled microwaveguides by changing the phase shift between the harmonic excitation signals applied to the two central channels of one of the layers, and by varying the magnitude of the vertical and lateral gaps. The mode of concentration power of the signal encoded in the form of amplitude and phase of the SW at the ends of the center channels with a the possibility of their separate inclusion, as well as the mode of signal control at the ends of microstrips the upper layer of the ensemble with the possibility of changing the phase of the output signal in a separate channel, that allows to use an array of microwaveguides as a controlled logical device or a multichannel power divider.

**Keywords:** spin wave, micromagnetic modeling, spin-wave beam, discrete diffraction.

DOI: 10.61011/PSS.2023.10.57218.157

### 1. Introduction

Transfer of the magnetic moment or electron spin instead of charge transfer opens new possibilities for using quanta of spin-wave excitations — magnons to develop methods and approaches for processing, transmitting and storing signals encoded in the form of amplitude and phase of spin waves (SW) [1,2] in the microwave and terahertz ranges [3,4]. In this case, the lengths of the excited SW range from hundreds of microns to tens of nanometers and can vary: by changing the magnitude and direction of the magnetization field, by varying the type and magnitude of anisotropy of the magnetic material, by irradiating the surface of magnetic films with focused laser radiation [5–9].

The unprecedented low attenuation of SW in YIG films is basis of the study discipline of spin transfer processes occurring in structured films, and studied within the framework of scientific discipline of physics of magnetic phenomena and condensed matter physics — dielectric magnonics [10]. In this case, YIG is used as materials and media for studying the processes determining the control of such SW characteristics as: the magnitude and direction of the group velocity, the spatial distribution of the amplitude and phase of SW, frequency ranges of SW excitation and propagation, the use of various methods to control SW coupling in multilayer structures and other [11]. A number of works shown the possibility of using YIG-based structures to demonstrate the principles of operation of logical devices in the microwave range. Planar ferrite

waveguide microstructures of finite width based on YIG can be used as basic elements of „magnon networks“ to create various signal processing devices: delay lines, filters, interferometers, switches, multiplexers, etc., in which information is transmitted via spin waves, and logical operations are implemented based on the principles of spin-wave interference. The use of lateral magnetic microstructures seems important for the development of interconnect elements in planar topologies of magnon networks [12,13]. Control of frequency tuning and of the output signal parameters in lateral microstructures with ferroelectric and piezoelectric layers [14–18] is carried out, for example, by changing the effective dielectric constant and permeability of a layered multiferroic structure during variations in external electric and magnetic fields, respectively. However, the construction of such structures requires precise matching when placing piezoelectric layers on the surface of YIG waveguides or during the ion-beam deposition of YIG on the surface of piezoelectric or semiconductor substrates [5,19–20]. The study of multilayer structures, each layer of which is formed by a system of microwaveguides, separated by an air gap and located on the same substrate, allows us to consider a method to control the spectra of spin waves and the propagation modes of the signal excited in the microwaveguides of one of the layers by changing the distance between individual waveguides and between layers of the system. This method to control the signal division between the structure channels expands the functionality of

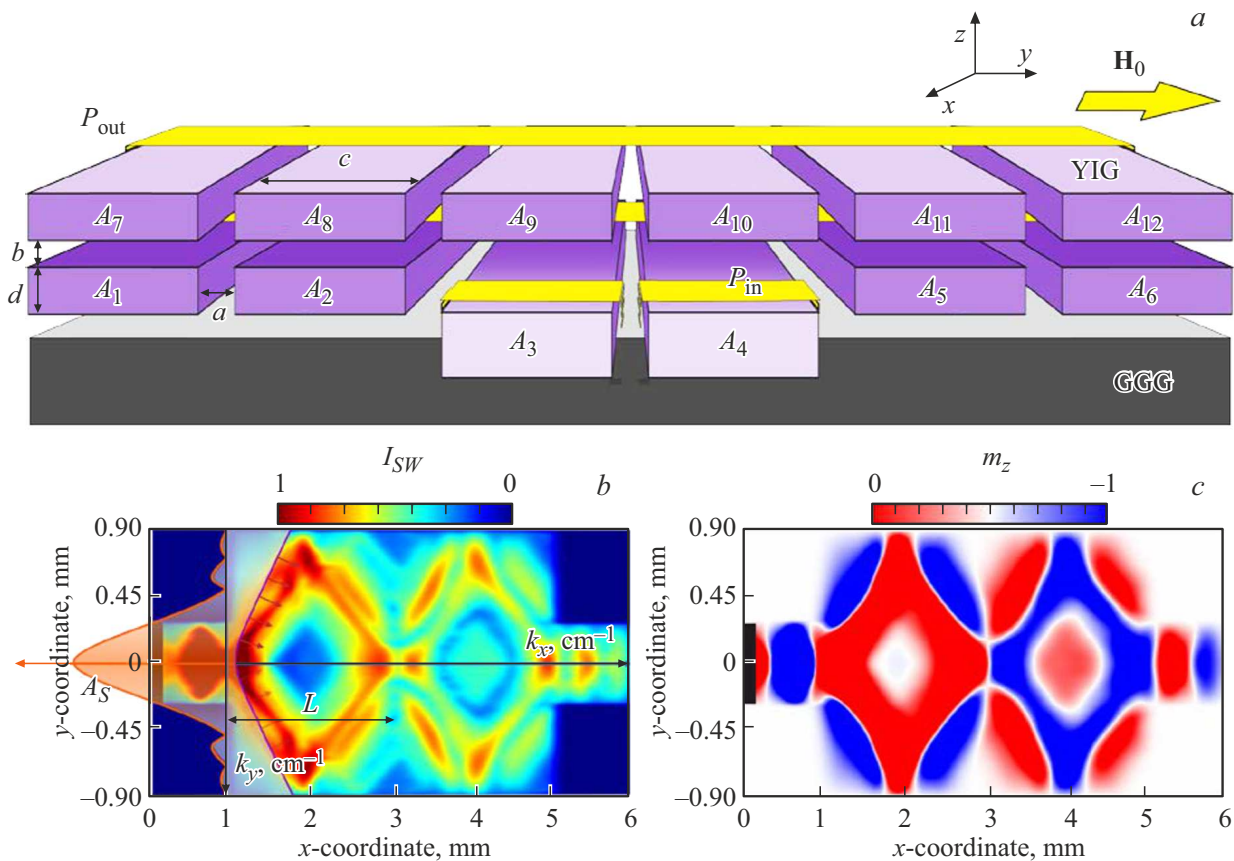


**Figure 1.** (a) Schematic illustration of an array of microwguides made from YIG films on GGG substrate. The following notations are introduced in the Figure:  $A_{1-12}$  — numbers microwave guides in array,  $a$  — vertical gap,  $b$  — horizontal gap,  $c$  — width,  $d$  — thickness,  $H_0$  — external magnetic field,  $P_{in}$  and  $P_{out}$  — microstrip antennas for SW excitation and reception, respectively. (b) Spatial distribution of SW intensity and curve reflecting the efficiency of excitation of SW transverse wave numbers, and isofrequency characteristic of SW for frequency of 5.25 GHz. (c) Map of the spatial distribution of the component  $m_z$  of dynamic magnetization for SW propagating in structure formed by one layer of YIG film.

magnon structures used in tasks of parallel processing of information signals.

In this paper the modes of propagation of spin waves in arrays of microwguides formed by two YIG layers were studied. The mechanisms leading to the formation of various „patterns“ formed by a spin-wave signal during its propagation in a system of longitudinally irregular thin-film magnon microwguides located in each layer of the structure have been studied. A study was carried out relating the geometric parameters influence on the characteristics of propagating SWs. Namely, the influence of the gap between the layers (in the vertical direction) and the gaps between individual ferrite microstrips on the formation of asymmetric „patterns“ of dynamic magnetization in each layer of the structure was considered.

## 2. Structure under study and numerical model

Micromagnetic modeling [21] was carried out for a system of laterally and vertically coupled ferrite microwave-

guides (Figure 1). YIG was chosen as the material. Microwguides are made in the form of elongated strips with length  $L = 4$  mm, width  $c = 300 \mu\text{m}$  and thickness  $d = 10 \mu\text{m}$ . The structure consists of two layers, each of which contains six parallel-oriented microwguides separated by the air gap. The YIG saturation magnetization is  $M = 139$  G, and the magnitude of the external magnetic field directed along the axis  $y$  is  $H_0 = 1200$  Oe. The numerical study was carried out at frequency of 5.25 GHz for all cases considered in this paper. In this case, this magnetization configuration provides effective excitation of surface spin waves (MSSWs). As it is known, the coupled ferrite structures expand the functionality of microwave devices due to an additional control parameter, which is the coupling between SW propagating in individual ferromagnetic films [22–26]. Note that in the experimental study of such structures YIG waveguides are formed on a substrate of gallium-gadolinium garnet (GGG) [27].

Considering one layer of the structure with a zero lateral gap, one can observe the SW diffraction mode in the region of junction of the microwguides of the input section with

width  $2c = 600 \mu\text{m}$  and of the main section of the structure with width  $6c = 900 \mu\text{m}$ . Figure 1, *b* for this case at the input signal frequency  $f = 5.25 \text{ GHz}$  shows the result of calculating the spatial distribution of the spin wave intensity

$$I_{SW}(x, y) = \sqrt{m_x^2(x, y) + m_y^2(x, y)},$$

where  $m_x, m_y$  — dynamic components of magnetization. Note that for a tangentially magnetized YIG film, during the propagation of the magnetostatic surface wave (MSSW) and diffraction on the region of junction of microwaveguides a mode of formation of two caustic beams of waves is observed, they propagate at angles  $\phi$  to the longitudinal axis  $x$  of structure (see Figure 1, *b*) [26,28–29]. In this case, the direction of the phase velocity is set by an antenna located in the input section of the microwaveguide with width of  $2c$ , and coincides with the direction of the axis  $x$ . The direction of the group velocity  $v_{gr}$  is determined by the normal to the isofrequency characteristic, shown by the dashed curve, at the point corresponding to the wave number  $\mathbf{k}$  with components  $(k_x, k_y)$ , as shown in Figure 1, *b*. Note that the range of transverse wave numbers is determined by the width of the input section and the maximum value of the excited transverse wave number is determined from the relation:  $[k_y]_{\max} = \pi/(2c)$ . To explain the determinations of the range of longitudinal and transverse wave numbers in the structure under consideration, Figure 1, *b* shows the calculated dependence of the magnitude of SW excitation amplitude on  $k_y$ . It can be seen that in the central region of the structure with width of  $6c$  the formation of two SW beams and their reflection from the boundaries of the structure are observed. In Figure 1, *b* the distance from the beginning of the microwaveguides junction region to the first waist of the spin-wave beam  $L = 2.0 \text{ mm}$  is introduced. SW propagation in the central part of the microstructure can also be described based on the concept of interference of transverse spin-wave modes. As can be seen from Figure 1, *c*, which shows the distribution of magnitude of the component  $m_z(x, y)$  of dynamic magnetization, a wave field distribution is formed in the cross section, the wave field is formed by an integer number of half-wavelengths  $3\Lambda/2$ , where  $\Lambda = 2\pi/k_y$ , from this we can conclude that the system exhibits interference of the first and third width modes with transverse wave numbers  $k_y^I = \pi/(6c)$  and  $k_y^{III} = \pi/(6c)$  and longitudinal wave numbers  $k_x^I = k_x^I(f)$  and  $k_x^{III} = k_x^{III}(f)$ , their frequency dependence is determined from the dispersion law for a plane-parallel ferrite waveguide of finite width [30,31]. The field amplitude can be described by the relation:

$$A(x, y) = a_I \Phi_I(y) \exp(-ik_x^I x) + a_{III} \Phi_{III}(y) \exp(-ik_x^{III} x),$$

where the functions  $\Phi_{I,III}(y)$  describe the transverse profile of the first and third width modes [32]. In this case, it can be shown that the characteristic distance between the positions of the field maxima on the longitudinal axis of the structure will be equal to a value called the coupling length and

determined by the relation:  $L = \pi/|k_x^{III} - k_x^I|$  [33]. In the range of excitation of magnetostatic surface waves, a change in the coupling length is observed, while the dependence  $L(f)$  has a monotonically increasing character, as shown in a number of papers [6,12,27]. Note that change in the lateral gap in the range from 10 to  $40 \mu\text{m}$  leads to change in the coupling length by 4 times [27] for the same spin wave frequency.

### 3. Results of micromagnetic modeling of spin wave propagation modes in array of YIG stripes

Let's move on to studying the method to control the spatial structure of the spin-wave beam and its division between channels in the array of laterally and vertically coupled SW waveguides. We will study the mode of SW power concentration at the ends of the middle channels with the possibility of their separate inclusion, as well as the signal control mode at the ends of the microstrips of the upper layer of the ensemble with the possibility of changing the output signal phase. In this case, we will consider the influence of excitation conditions and the magnitude of the vertical and lateral gap on the position of the waist of the spin-wave beam when two layers consisting of YIG microwaveguides, shown in Figure 1, *a*, are introduced into the structure.

Let us consider the operation principle of the structure under study. The microwave signal  $P_{in}$  is supplied to the input antennas located on the microwaveguides  $A_{3,4}$ . The structure was excited by creating a localized region with an alternating external magnetic field on two central microwaveguides in one of the layers. The dynamic properties of wave processes change due to the coupling between SW propagating in individual layers and channels of the two-layer structure. Numerical modeling of modes of SW propagation in the array of YIG microwaveguides was carried out based on the solution of Landau–Lifshitz–Gilbert (LLG) equation [34]. Two cases of SW excitation at sources are considered: in-phase (see Figure 2, *a, b*) for the lower layer, for the upper layer (Figure 2, *c, d*) and the case of antiphase excitation in Figure 2, *e, f* of the lower layer and Figure 2, *g, h* of the upper layer of microwaveguides. As SW propagates, there is a „pumping“ of the spin-wave signal into all microwaveguides, depending on the phase difference of the microwave signal supplied to the input antennas.

Figure 2, *a–d* shows in-phase excitation, when the magnitude of the lateral and vertical gaps is  $10 \mu\text{m}$ , the SW intensity has maximum in two central channels, at  $x = 3.8 \text{ mm}$ . In this case, one can observe intensity redistribution from two central channels  $A_{3,4}$  to the side ones  $A_{1,2,5,6}$ . On the lower layer of the structure, where the excited waveguides are located, the localization of the SW power is observed in the region of the output sections of the central channels  $A_{3,4}$  (see Figure 2, *a, b*). It is clear that in the input and output regions of the central channels  $A_{3,4}$

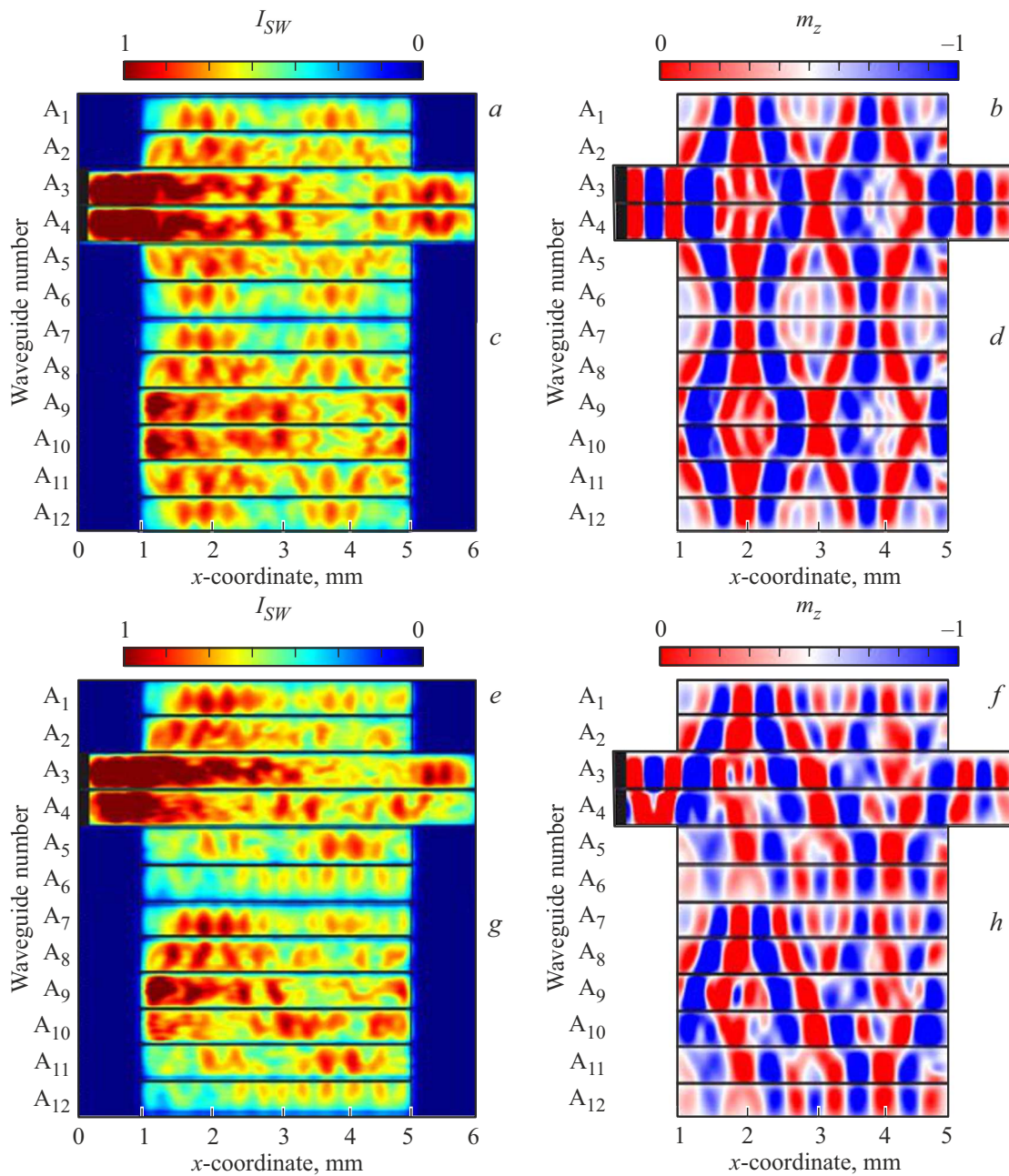


**Figure 2.** Results of calculation of stationary SW profile in each of the layers of the structure for two types of excitation of the input central microwaveguides. (a, c, e, g) Spatial distribution of SW intensity. (b, d, f, h) Maps of the spatial distribution of  $m_z$  dynamic magnetization component for SW propagating in array of microwaveguides, where the lateral and vertical gap is  $10\ \mu\text{m}$ . The calculation results are given for the input signal frequency of 5.25 GHz and magnetic field of 1200 Oe.

SW length is  $500\ \mu\text{m}$ , which corresponds to the calculation of the symmetric mode dispersion of the lateral structure with the given geometric dimensions [27].

In the case of antiphase excitation in Figure 2, e–h the SW propagation has asymmetric profile of the spin-wave beam on the upper layer of the structure in the waveguides A<sub>7–9</sub> (see Figure 2, g). In the output sections of the microwaveguides, one can observe the localization of SW power at  $x = 5.5\ \text{mm}$ , namely the intensity maximum in A<sub>3</sub> and vice versa the minimum in A<sub>4</sub>.

When the lateral and vertical gaps increase by 2 times when  $a = b = 20\ \mu\text{m}$ , the effective pumping of the spin-wave signal into the upper layer of the structure is observed. In this case, the signal does not enter the waveguides A<sub>1,6</sub> on the bottom layer and A<sub>7,12</sub> on the top layer. In the case of in-phase excitation the energy of same power propagates in the lower layer, and in the case of anti-phase excitation it propagates only in the central microwaveguides.

When comparing the results of numerical modeling for the array of microwaveguides with dimension of  $2 \times 6$  in

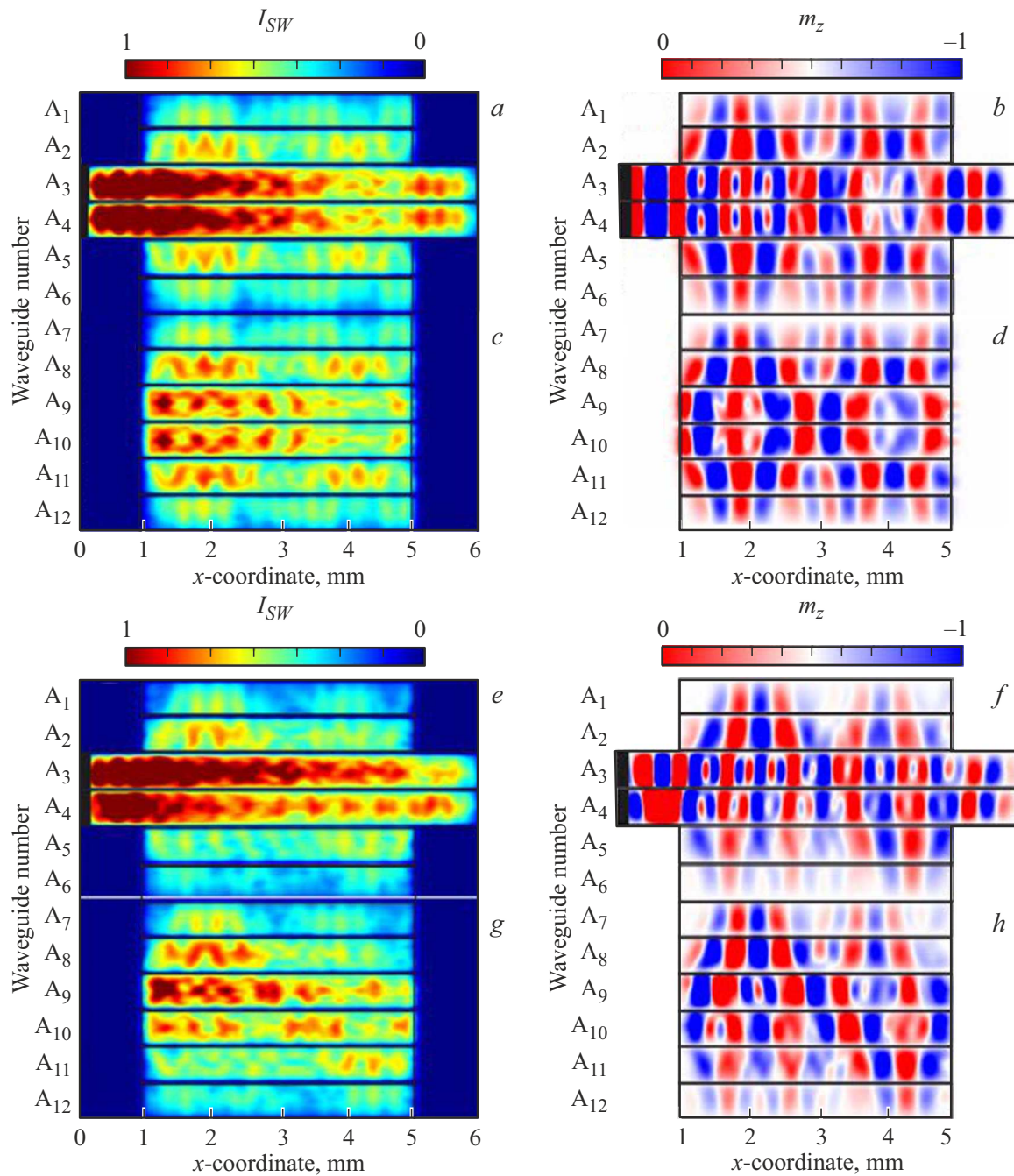


**Figure 3.** Results of calculation of SW propagation modes in array of microwaveguides in each of the layers of the structure for two types of excitation of the input central microwaveguides with lateral and vertical gaps of  $20\ \mu\text{m}$ . (a, c, e, g) Spatial distribution of SW intensity. (b, d, f, h) Maps of the spatial distribution of component  $m_z$  of dynamic magnetization for SW.

Figures 2 and 3 at the same values of the lateral and vertical gaps equal to 10 and  $20\ \mu\text{m}$  respectively, the change in the magnitude of the coupling between the microwaveguides is observed, which affects the power redistribution to adjacent channels of the structure. Note that when comparing the case of in-phase excitation in Figures 2 and 3, we can see increase in the distance  $L$  along the axis  $x$  by 0.2 mm.

In the array of microwaveguides in Figure 4 the lateral gap is  $20\ \mu\text{m}$ , and the vertical gap is  $10\ \mu\text{m}$ . With

such geometric dimensions in the structure under in-phase excitation, Figure 4, a from the beginning of the region of junction of the microwaveguides to the first waist of the spin-wave beam  $L = 2.8\ \text{mm}$ , in contrast to the single-layer film in Figure 1, b.

Comparing the lower and upper layers in the case of antiphase excitation in Figure 4, e, f, the intensity redistribution is observed, namely, SW powers are transmitted from the two central channels  $A_{3,4}$  to the side  $A_{1,2,7,8}$ .

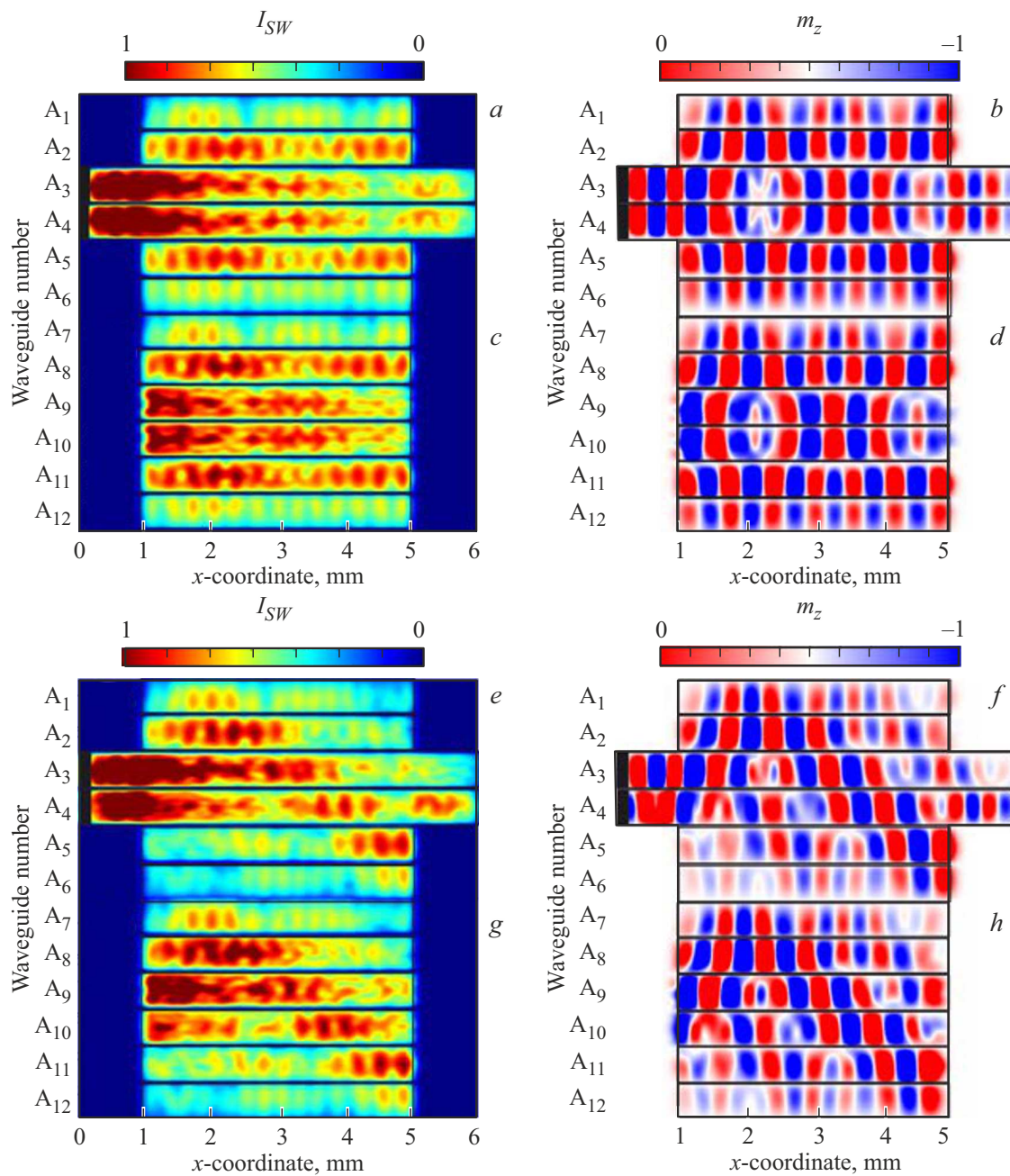


**Figure 4.** (a, c, e, g) Spatial distribution of SW intensity. (b, d, f, h) Maps of spatial distribution of component  $m_z$  of dynamic magnetization for SW propagating in array of microwaveguide array, where the lateral gap is  $20\ \mu\text{m}$ , vertical —  $10\ \mu\text{m}$ .

On the lower layer of the structure, where the excited waveguides are located, the localization of the SW power is observed in the region of channel A<sub>4</sub> (see Figure 4, e) at  $x = 5.5\ \text{mm}$ . In the case of antiphase excitation in Figure 4, e–h, SW propagation occurs with phase shift between the layers, namely, the position of the zero value of the spatial distribution of  $m_z$  component of the dynamic magnetization in the excited layer and the second layer is shifted by  $200\ \mu\text{m}$  at spin wavelength of  $500\ \mu\text{m}$ .

In this variant of the structure configuration it is clear that in the central region the formation of two SW

beams is observed, at distance from the beginning of the microwaveguides junction region to the first waist of the spin-wave beam  $L = 2.3\ \text{mm}$ .

It was also revealed that as the vertical gap increases, the signal intensity distribution between the first and second layers of the microwaveguide system becomes less and less identical, while the value of the parameter  $L$  in each layer of the structure has a different value. Thus, we obtain two modes of spin-wave transport: a mode of SW concentration on the output sections of the central channels A<sub>3,4</sub>, with the possibility of their separate inclusion, as well

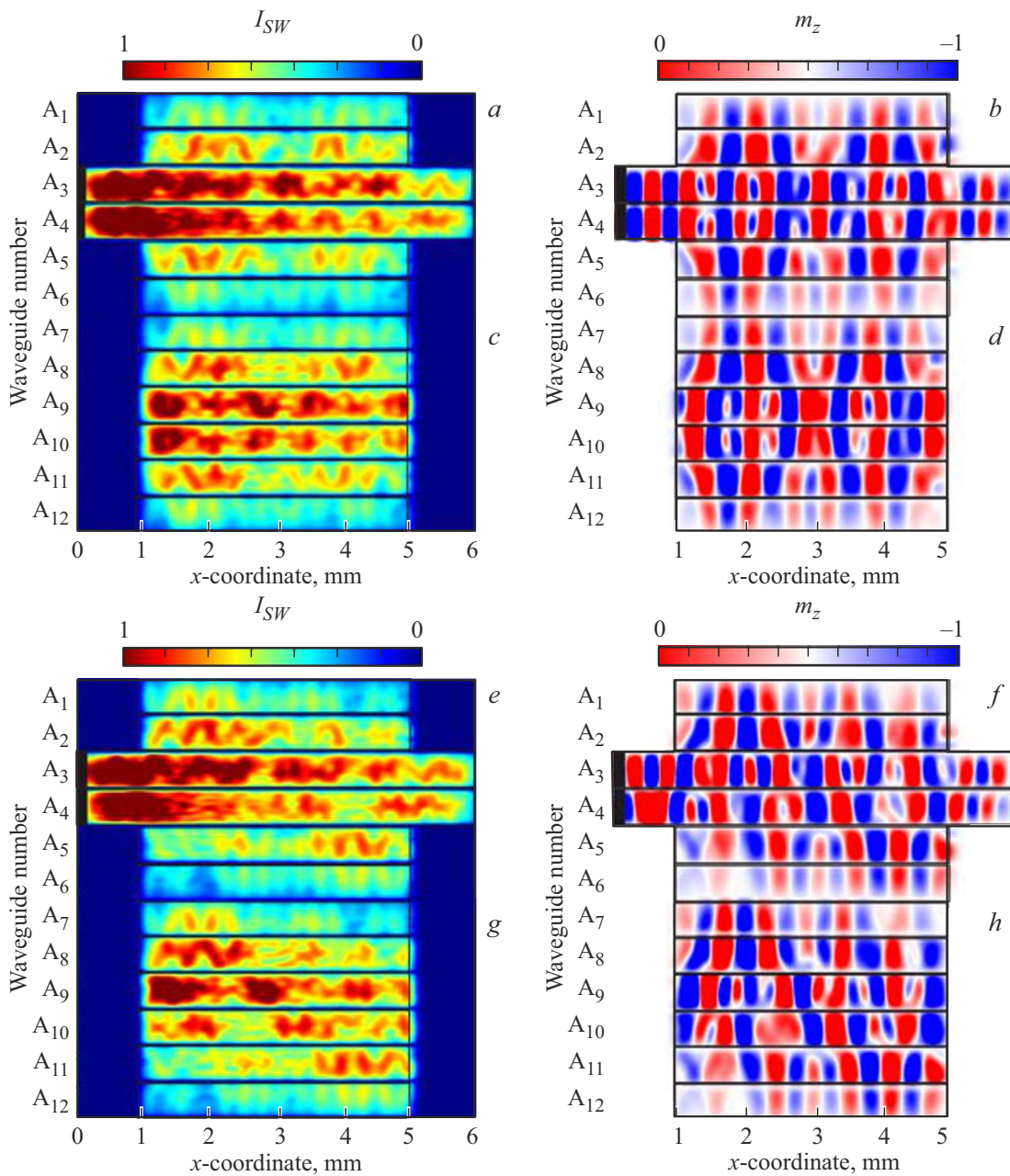


**Figure 5.** *a, c, e, g* — spatial distribution of SW intensity; *b, d, f, h* maps of the spatial distribution of component  $m_z$  of dynamic magnetization for SW propagating in array of microwaveguides, where the lateral gap is  $20\ \mu\text{m}$ , vertical —  $40\ \mu\text{m}$ .

as signal control mode with the possibility of changing the output signal phase. Thus, in the lower layer of the structure three modes can be observed in the output sections of microwaveguides  $A_{3,4}$  at  $x = 5.5\ \text{mm}$ : the first in Figure 2, *e*, where the maximum energy falls on the waveguide  $A_3$ , the second in Figure 4, *e* where the maximum can be obtained on the channel  $A_4$ . The third case is when in both channels  $A_{3,4}$  at  $x = 5.5\ \text{mm}$  the same value of SW intensity is observed. As noted in Section 2, the change in the lateral gap leads to change in the coupling length. A similar statement is true for the vertical gap, at that when considering the effects of dipole coupling of spin

waves in the vertical direction, the increase in the air gap leads to an increase in the coupling length [1,10,22–24].

Thus, analyzing the maps obtained during micromagnetic modeling for the spatial distribution of magnetization with different types of SW excitation, the possibility to control the transverse structure of the spin wave field in each layer and in the output sections of the structure was shown. The structure under consideration based on the array of YIG microwaveguides can be used to create multichannel signal separation systems, which can be implemented by placing antennas in the region of the outputs of each of the microwaveguides.

## 4. Conclusion

This paper discusses methods to control the characteristics of spin-wave signal based on signal changes at the source in in-phase and anti-phase signals on two central microwaveguides. Using micromagnetic modeling, the modes of SW propagation in arrays of microwaveguides formed by YIG strips are studied. The influence of the method of excitation of the array of microwaveguides on the profiles of the spin-wave signal and the effective redistribution of SW power in each of 12 channels of the structure under consideration is identified. In configuration corresponding to the in-phase and antiphase method of excitation of the two central channels of the lower layer of surface magnetostatic spin waves, it is possible to observe a non-identical distribution of the magnitude of the dynamic magnetization in each layer when the orientation of the direction of the external magnetic field changes. Thus, the proposed structure can be used for efficient filtering and processing of signals in various applications related to magnetic microelectronics and spintronics.

## Funding

This study was financially supported by the Russian Science Foundation under project No. 23-79-30027.

## Conflict of interest

The authors declare that they have no conflict of interest.

## References

- [1] S.A. Nikitov, D.V. Kalyabin, I.V. Lisenkov, A.N. Slavin, Y.N. Barabanenkov, S.A. Osokin, A.V. Sadovnikov, E.N. Beginin, M.A. Morozova, Y.P. Sharaevsky, Y.A. Filimonov, Y.V. Khivintsev, S.L. Vysotsky, V.K. Sakharov, E.S. Pavlov. *Phys. Usp.* **58**, 10, 1002 (2015).
- [2] V.E. Demidov, S. Urazhdin, A. Zholud, A.V. Sadovnikov, A.N. Slavin, S.O. Demokritov. *Sci. Rep.* **5**, 8578 (2015).
- [3] C.S. Davies, A. Francis, A.V. Sadovnikov, S.V. Chertopalov, M.T. Bryan, S.V. Grishin, D.A. Allwood, Y.P. Sharaevskii, S.A. Nikitov, V.V. Kruglyak. *Phys. Rev. B* **92**, 020408(R) (2015).
- [4] A.V. Chumak, V.I. Vasyuchka, A.A. Serga, B. Hillebrands. *Nature Phys.* **11**, 453 (2015).
- [5] A.V. Sadovnikov, S.A. Nikitov, E.N. Beginin, S.E. Sheshukova, Yu.P. Sharaevskii, A.I. Stognij, N.N. Novitski, V.K. Sakharov, Yu.V. Khivintsev. *Phys. Rev. B* **99**, 054424 (2019).
- [6] A.V. Sadovnikov, A.A. Zyablovsky, A.V. Dorofeenko, S.A. Nikitov. *Phys. Rev. Appl.* **18**, 024073 (2022).
- [7] M. Balynsky, D. Gutierrez, H. Chiang, A. Kozhevnikov, G. Dudko, Y. Filimonov, A.A. Balandin, A. Khitun. *Sci. Rep.* **7**, 11539 (2017).
- [8] A.B. Ustinov, A.V. Drozdovskii, B.A. Kalinikos. *Appl. Phys. Lett.* **96**, 142513 (2010).
- [9] L.A. Shelukhin, V.V. Pavlov, P.A. Usachev, P.Yu. Shamray, R.V. Pisarev, A.M. Kalashnikova. *Phys. Rev. B* **97**, 014422 (2018).
- [10] S.A. Nikitov, A.R. Safin, D.V. Kalyabin, A.V. Sadovnikov, E.N. Beginin, M.V. Logunov, M.A. Morozova, S.A. Odintsov, S.A. Osokin, A.Yu. Sharaevskaya, Yu.P. Sharaevskiy, A.I. Kirilyuk. *UFN*, **190**, 1009 (2020). (in Russian).
- [11] A. Chumak. *IEEE Trans. Magn.* **58**, 6 (2022).
- [12] A.V. Sadovnikov, E.N. Beginin, S.A. Odincov, S.E. Sheshukova, Yu.P. Sharaevskii, A.I. Stognij, S.A. Nikitov. *Appl. Phys. Lett.* **108**, 172411 (2016).
- [13] A.Yu. Annenkov, S.V. Gerus, S.I. Kovalev. *ZhTF* **68**, 91 (1998). (in Russian).
- [14] Y.K. Fetisov, G. Srinivasan. *Appl. Phys. Lett.* **88**, 14 (2006).
- [15] S.L. Vysotsky, Yu.V. Khivintsev, V.K. Sakharov, Yu.A. Filimonov. *ZhTF* **89**, 1044 (2019). (in Russian).
- [16] A.B. Ustinov, A.V. Drozdovskii, A.A. Nikitin, A.A. Semenov, D.A. Bozhko, A.A. Serga, B. Hillebrands, E. Lähderanta, B.A. Kalinikos. *Commun. Phys.* **2**, 1, 137 (2019).
- [17] A.A. Grachev, A.V. Sadovnikov, S.A. Nikitov. *Nanomater.* **12**, 9, 1520 (2022).
- [18] A.V. Sadovnikov, A.A. Grachev, E.N. Beginin, S.A. Odintsov, S.E. Sheshukova, Yu.P. Sharaevsky, S.A. Nikitov. *Pis'ma v ZhETF* **105**, 6, 347 (2017). (in Russian)
- [19] A. Stognij, L. Lutsev, N. Novitskii, A. Bespalov, O. Golikova, V. Ketsko, R. Gieniusz, A. Maziewski. *J. Phys. D* **48**, 485002 (2015).
- [20] A.I. Stognij, L.V. Lutsev, V.E. Bursian, N.N. Novitskii. *J. Appl. Phys.* **118**, 023905 (2015).
- [21] G. Gubbiotti, A. Sadovnikov, E. Beginin, S. Nikitov, D. Wan, A. Gupta, S. Kundu, G. Talmelli, R. Carpenter, I. Asselberghs, I.P. Radu, C. Adelman, F. Ciubotaru. *Phys. Rev. Appl.* **15**, 014061 (2021).
- [22] A.K. Ganguly, C. Vittoria. *J. Appl. Phys.* **45**, 4665 (1974).
- [23] H. Puzskarski. *Surf. Sci. Rep.* **20**, 45 (1994).
- [24] M.R. Daniel, P.R. Emtage. *J. Appl. Phys.* **53**, 3723 (1982).
- [25] B. Hillebrands. *Phys. Rev. B* **41**, 530 (1990).
- [26] A.V. Vashkovsky, V.S. Stalmakhov, Yu.P. Sharaevsky. *Magnitostatichekie volny v elektronike vysokikh chastot. Izd-vo Saratov. un-ta, Saratov* (1993). 314 s. (in Russian).
- [27] A.V. Sadovnikov, E.N. Beginin, S.E. Sheshukova, D.V. Romanenko, Yu.P. Sharaevskii, S.A. Nikitov. *Appl. Phys. Lett.* **107**, 202405 (2015).
- [28] A.Y. Annenkov, S.V. Gerus, E.H. Lock. *Europhys. Lett.* **123**, 44003 (2018).
- [29] A.B. Khutueva, A.V. Sadovnikov, A.Yu. Annenkov, S.V. Gerus, E.G. Locke. *Izv. RAN. Ser. fiz.* **85**, 11, 1542 (2021). (in Russian).
- [30] S.N. Bajpai. *J. Appl. Phys.* **58**, 910 (1985).
- [31] T.W. O'Keeffe, R.W. Patterson. *J. Appl. Phys.* **49**, 4886 (1978).
- [32] O. Buttner, M. Bauer, C. Mathieu, S.O. Demokritov, B. Hillebrands, P.A. Kolodin, M.P. Kostylev, S. Sure, H. Dotsch, V. Grimalsky, Y. Rapoport, A.N. Slavin. *IEEE Trans. Magn.* **34**, 1381 (1998).
- [33] V.E. Demidov, S.O. Demokritov, K. Rott, P. Krzysteczko, G. Reiss. *Appl. Phys. Lett.* **91**, 252504 (2007).
- [34] A. Vansteenkiste, J. Leliaert, M. Dvornik, M. Helsen, F. Garcia-Sanchez. *AIP Adv.* **4**, 107133 (2014).

Translated by I.Mazurov